Canadian Solar Buildings Conference
Montreal, August 20-24, 2004
Refereed Paper

OPTICAL, ELECTRICAL AND STRUCTURAL PROPERTIES OF PECVD QUASI EPITAXIAL PHOSPHOROUS DOPED SILICON FILMS ON CRYSTALLINE SILICON SUBSTRATE

Mahdi Farrokh-Baroughi, Hassan El-Gohary, and Siva Sivoththaman
Department of Electrical & Computer Engineering, University of Waterloo
200 University Avenue West, Waterloo, Ontario N2L 3G1, Canada.

ABSTRACT

We have developed highly conductive silicon emitters using plasma enhanced chemical vapor deposition (PECVD) of highly hydrogen-diluted silane and phosphine on crystalline silicon substrates. High resolution transmission electron microscope images show a perfect long range crystalline silicon order at the first few tens of nanometers of the film thickness. In higher thicknesses, however, a slowly varying shorter range order was observed. The comparison of the film conductivities on glass (10 $\Omega^{-1}cm^{-1}$- 20 $\Omega^{-1}cm^{-1}$) and on c-Si substrates (110 – 450 $\Omega^{-1}cm^{-1}$) confirms an improved doping efficiency and carrier mobility due to the higher crystallinity in the films deposited on the c-Si substrates. The optical properties of the films were assessed by quantum efficiency measurements on test solar cells.

INTRODUCTION

Silicon-based thin films such as amprphous and microcrydtalline (Poissant et al., 2003) films have been extensively studied for solar cell applications. It has been shown recently that the direct PECVD of a thin intrinsic Si film on a crystalline silicon (c-Si) using highly hydrogen diluted silane results in a quasi-epitaxial (qEpi) growth of Si film where the deposited film follows the crystal order of the substrate (Pla et al., 2002). Such films have been recently employed as intrinsic buffer layer in a heterojunction solar cell structure (Centurioni et al., 2004). However, to the best of our knowledge, q-Epi growth of highly doped highly conductive emitters has not been reported. This paper presents a new highly conductive (n^+) Si emitter for PV application. The obtained conductivity values in the range of 100 $\Omega^{-1}cm^{-1}$–450 $\Omega^{-1}cm^{-1}$ fall into the category of high temperature diffusion emitters (Kerr et al., 2001) rather than low temperature (LT) PECVD emitters (Saha et al., 1997, Alpuim et al., 2003). These emitters provide a new work frame for LT Si solar cells. This makes the use of simple solar cell structures without transparent conductive oxides possible (Farrokh-Baroughi et al., 2006). This paper presents the structural, electrical and optical properties of the qEpi-Si films.

EXPERIMENTAL

Films with different thicknesses were employed in this study on three kinds of substrates: CZ - Si wafers with resistivity of 8-12 Ω.cm, multicrystalline Si substrates (mc-Si) with resistivity of 1-2 Ω.cm, and glass wafers.

For TEM analysis, we used the mc-Si wafers with random crystal orientations to investigate the structure of the deposited films and the orientation dependence of the deposition rates. The CZ, mc-Si and glass substrates were employed in conductivity measurements. For optical characterization of the developed films some test solar cells were fabricated on mc-Si substrates.

Since the deposited films follow the crystalline order of the c-Si substrates, the clean and oxide-free surface is crucial to achieve a high crystallinity in the deposited film. We cleaned the Si substrates using RCA cleaning processes and performed an HF dip for 15 sec in 1% HF solution right before the loading of the wafers into the PECVD chamber. The hydrogen bonds on wafer surface formed during the HF dip prevent the formation of the native oxide during the short period of the wafer handling and pumping processes. (n^+) qEpi-Si films of different thicknesses with the deposition conditions listed in table 1 were deposited on the substrates. To prepare the samples for conductivity measurements, a two mask process was employed to pattern the active (n^+) region and the electrical contacts. The Al/(n^+)qEpi-Si/Al structure was used for the conductivity measurements and the Al/(n^+)qEpi-Si/(p)mc-Si/Al structure was employed as test photodiode for optical characterization of the film. The front side and the backside Al layers of 0.5µm thickness were deposited using RF magnetron sputtering.

HANWHA 1062

Table 1
Process conditions for the deposition of qEp-Si films on c-Si substrates

PH3/SIH4/H2	RF POWER	PRESSURE
0.04/4/500 sccm	70 mW/cm^2	900 mT

MEASUREMENT RESULTS AND DISCUSSION

Structural properties of the (n^+) qEpi-Si

The important structural aspects of the (n^+) qEpi-Si films are the substrate and crystal orientation dependence of the deposition rate, the quality of the interface between the deposited film and the underlying c-Si substrate, and the quality of the bulk of the deposited film. We have employed HRTEM analysis for structural study of the (n^+) qEpi-Si films.

As the first application of the HRTEM images, we compared the deposition rate of the qEpi-Si films on c-Si and glass substrates. Because of the similar physical properties of the qEpi-Si and c-Si materials it is not possible to selectively etch the qEpi-Si film on the c-Si substrate. TEM pictures, however, are able to show the difference between two materials. Furthermore, since the growth mechanisms of the qEpi-Si film using process parameters of table 1 on glass and c-Si substrate are different, epitaxial growth versus nc-Si growth, the deposition rates can be potentially different on these two substrates. Therefore, we designed an experiment to investigate this matter.

The deposition rate of 2.05 nm/min was measured on glass under the qEpi-Si process conditions listed in table 1. Figure 1(a) shows the TEM picture of a (n^+) qEpi-Si /mc-Si cross-section covered by a silicon nitride capping layer. The (n^+) qEpi-Si film in this structure was obtained by 45 min PECVD of the Si film using process parameters of table 1. The film thickness in the TEM picture is about 90 nm which is in good agreement with the predicted film thickness from the measured deposition rate on a glass substrate. Another important aspect of the deposition is the dependence of the deposition rate to the crystal orientation. Figure 1(a) and 1(b) show the qEpi-Si films of different thicknesses deposited on mc-Si wafers with random crystal orientations. A grain boundary (GB) and two twin boundaries (TBs) are visible in figure 1(a) and 1(b). It should be noted that the crystal orientation on the two sides of a GB or a TB are different. Since the film thickness in both figures is the same on different sides of the GB and TBs, we conclude that the deposition rate is not sensitive to the crystal orientation. As a result, we think that the deposition rates on c-Si wafers with different crystal orientations are close to the deposition rates on glass substrate.

The quality of the interface between the (n^+) qEpi-Si film and the c-Si substrate plays an important role in the quality of the PV cells based on these junctions. Figure 2(a) shows the HRTEM picture of the interface of a (n^+) qEpi-Si/(p)mc-Si junction. As shown in the figure, the deposited film in the interface and close to the interface shows a long range order similar to the long range order of the c-Si substrate. This supports the idea of quasi-epitaxial growth of the deposited film at LTs. Meanwhile, the figure shows that there is not a well-defined boundary between the deposited qEpi-Si film and the c-Si substrate and there is just a very thin transition region between the two materials. The high crystallinity of the film in the interface and close to the interface suggests that the electronic quality of the film in this region is good.

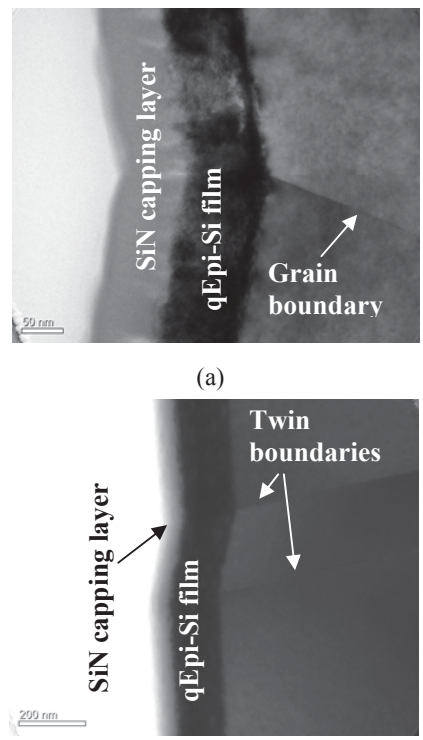

Figure 1. TEM cross-section of a SiN / (n^+) qEpi-Si / mc-Si structure (a) at the vicinity of a GB and (b) at the vicinity of two twin boundaries.

Figure 2(b) shows that the qEpi-Si film has followed the crystal orientation of the substrate up to at least 30nm. Although these figures show that the deposited film follows the substrate orientation to some extent, figure 2(c) shows that the long range order in the deposited film was lost in higher thicknesses. Lattice images at different directions far

from the interface are observable in figure 2(c). This suggests that the quality of the film decays at higher thicknesses. However, looks like at least in less than 100 nm thick films the changes is the crystal orientations is smooth and there are not sharp grain boundaries in the film. This is an important point that differentiates the LT qEpi-Si film from the nc-Si film.

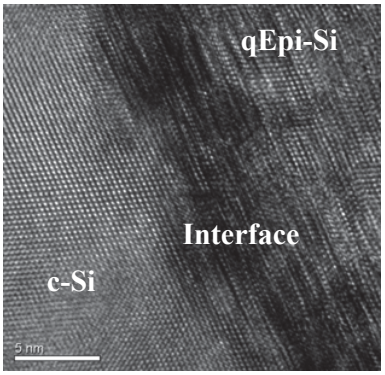

(a)

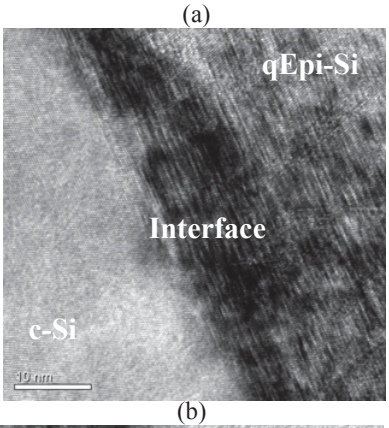

(b)

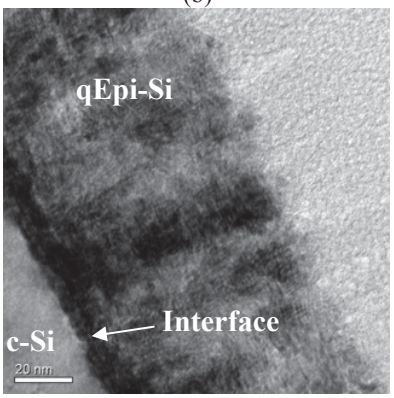

(c)

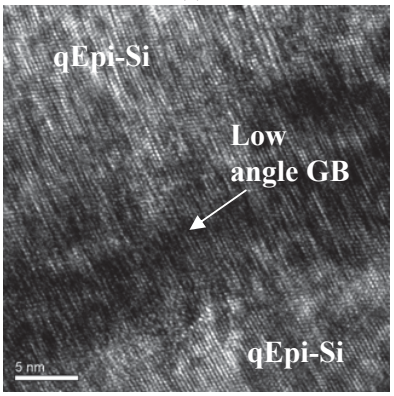

(d)

Figure 2: HRTEM picture of the qEpi-Si and c-Si (a) at the interface region in 5 nm scale, (b) at the interface region in 10 nm scale, (c) qEpi-Si film of 90nm thickness on the mc-Si substrate, and (d)bulk of the qEpi-Si at the vicinity of a low angle grain boundary within the film

This major difference between the two films originates from the substrate effect. Unlike nc-Si films on glass that the crystallites start at a point in an a-Si phase and grow over thickness, the crystallites of the qEpi-Si film grow directly on the c-Si substrate with the same crystal orientation without experiencing any incubation layer. In other words the c-Si acts as a crystal seed layer for the growth of the qEpi-Si film. The qE-Si film loses its crystallinity because of the LT nature of the process. Nonetheless, changes in the crystal orientations far from the c-Si substrate are expected to be smooth because crystallites start with the same orientations. Figure 2(d) shows a smooth change in crystal orientation deep inside of the qEpi-Si film.

Electrical properties of the (n^+) qEpi-Si

Electrical conductivity of the emitter depends on two parameters: the carrier mobility and the active doping density. Unlike high yemperature (HT) Si emitters obtained by diffusion of dopants in single c-Si wafers, the LT Si emitters normally have low conductivities (Alpuim et al., 2003). A good quality (n^+) a-Si has a conductivity of 0.01 $\Omega^{-1}cm^{-1}$ (Street, 1991) and a good quality thin (n^+) nc-Si has a much higher conductivity of 10-20 $\Omega^{-1}cm^{-1}$ [4]. It is known that during the deposition of a-Si at LT, most of the dopant (phosphorous in n-type material) atoms prefer to form three fold bonds (electrically inactive states) rather than 4 fold bonds (electrically active donor state). This highly reduces the doping efficiency [7]. For example, the doping efficiency of (n^+) a-Si film with 1% phosphine concentration in gas phase is about 1%. Although the doping efficiency in a nc-Si film is much higher than that of a-Si, the presence of a-Si tissues in this material especially at the incubation layer lowers the doping efficiency for a thin film. The only key to obtain highly conductive Si emitters using PECVD at LTs is to improve the crystallinity of the deposited films because the higher the crystallinity the higher the doping efficiency and carrier mobility. The thin (less that 100nm thickness) (n^+) Si films in this work show an outstanding crystallinity throughout the film. As the TEM pictures suggest, the films have the best crystallinity at the interface and close to the interface and have less crystallinity far from the interface. Nonetheless, the crystallinity far from the interface is still good and amorphous tissues are not observed in the films. As a result, higher conductivities are expected in qEpi-Si emitters. In order to measure the conductivity of the films, we deposited the qEpi-Si films with different thicknesses on glass and CZ-Si wafers and measured the sheet resistance of the films using simple electrical test structures. The conductivities of the films were calculated using the sheet resistance value and the thickness values of the films that were measured on the glass substrates. The major assumption in the electrical characterization was that the space charge region in (n^+) emitter is much thinner than the film thickness. We will show that this is a valid assumption.

Figure 3 shows the conductivities of the films of different thicknesses deposited on CZ substrates with (100) orientation and glass substrates using the deposition conditions of table 1. The experiments reveal three major differences between the qEpi-Si films on CZ-Si and the nc-Si films on glass: (i) the conductivity of the qEpi-Si films are at least one order of magnitude larger than the conductivity of the nc-Si films, (ii) the conductivity of both films depend on the films thickness, and (iii) the thickness dependence of the films on the two substrates show an opposite behavior. The conductivity of the qEpi-Si films decreases by increasing the film thickness and the conductivity of the nc-Si films increases by increasing the film thickness.

The huge difference in the conductivity of the films originates from higher crystallinity of the qEpi-Si films on the c-Si substrates. The thickness dependence of the conductivity of the qEpi-Si films suggest that the crystallinity and hence the doping efficiency and the carrier mobility of the qEpi-Si film decreases far from the interface region. This is consistent with the results of the structural studies in the previous section. On the other hand, thickness dependence of the nc-Si conductivity shows that the crystallinity of the film gets better at higher thickness. This is a well known phenomenon that is observed on nc-Si films developed on glass substrates (Luysberg et al., 1997). The observations here pinpoint to the major structural difference of the qEpi-Si film with normal nc-Si films. This result is consistent with our observations from the TEM analysis in the previous section.

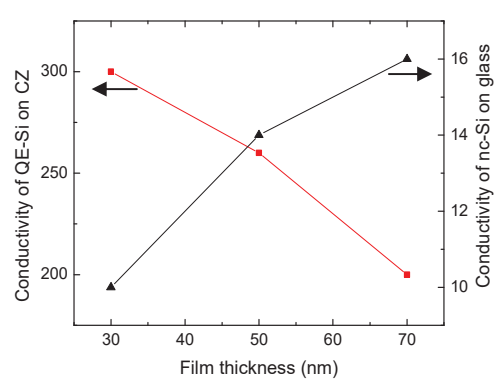

Figure 3. Conductivity of the deposited films on CZ-Si wafer and glass in $\Omega^{-1}cm^{-1}$.

To better understand the electrical properties of the qEpi-Si, the conductivity of the films are discussed here in more details. The conductivity of our (n^+)

qEpi-Si films developed at LT using PECVD technique falls in the range of 100 $\Omega^{-1}cm^{-1}$ to 450 $\Omega^{-1}cm^{-1}$. In addition, the conductivity of highly doped single c-Si wafers is normally between 100 and 1000 $\Omega^{-1}cm^{-1}$. Therefore, we assume that a thin qEpi-Si film has the same material parameters of a single c-Si material and we assess the conductivity.

Consider an (n^+) Si film with a conductivity of 100 – 450 $\Omega^{-1}cm^{-1}$ with phosphorous concentration of NPh and an active donor concentration of N_D. The material is highly degenerate; therefore the Fermi-Dirac integral should be employed for finding the free electron concentration. The charge neutrality in this film reduces to $N_D^+ = n_0$ where N_D^+ and n_0 are the ionized active donor density and free electron density, respectively.

The free electron concentration and the density of ionized donor states in the film are given by,

$$n_0 = \frac{2N_C}{\sqrt{\pi}} F_{1/2}\left(\frac{E_F - E_C}{kT}\right) \qquad (1)$$
$$N_D^+ = N_D\left(1 - f(E_D)\right)$$

where the E_C, E_F, N_C, E_C, $F_{1/2}$, f, k and T are conduction band edge, , Fermi energy, effective density of states in the conduction band edge, Fermi integral, Fermi-Dirac distribution function, Boltzman constant, and temperature, respectively.

Substituting n_0 and N_D^+ in the charge neutrality and simplifying the expression we obtain the relationship between N_D and the position of the Fermi level.

$$N_D = \left(1 + e^{-\frac{E_D - E_F}{kT}}\right) \times \frac{2N_C}{\sqrt{\pi}} \times \int_0^\infty \frac{\sqrt{\eta}}{1 + \exp(\eta - \frac{E_F - E_C}{kT})} d\eta \qquad (2)$$

where E_D is the energy level of the phosphorous dopant atoms in the c-Si bandgap. Figure 4 is the plot of N_D and n_0 obtained versus the Fermi-level energy respect to E_{C0} (the conduction band edge of the c-Si material without considering bandgap narrowing) normalized to the thermal potential. Since the bandgap narrowing affects the charge concentration at high doping densities, we have calculated the curves with 0, 0.05 eV and 0.1 eV bandgap narrowings at the conduction band.

The gas phase phosphorous to silicon concentration ratio during depositing (n^+) qEpi-Si film was 0.01. If an equal gas phase and solid phase phosphorous to silicon ratio is assumed, the phosphorous concentration in the film becomes $5x10^{20}$ cm^{-3}. The value of N_D becomes equal to $5x10^{20}$ cm^{-3} and $2.5x10^{20}$ cm-3 for a 100% and 50% doping efficiencies, respectively. For N_D of $5x10^{20}$ cm^{-3} the n_0 in the range of $3x10^{19}$ cm-3 to $9x10^{19}$ cm^{-3} is obtained from figure 4. Table 2 lists the estimated mobility values for the films with conductivities in the range of 100 – 450 $\Omega^{-1}cm^{-1}$ assuming typical values for N_D and bandgap narrowing. The estimated electron mobility values without considering the bandgap narrowing for such highly doped material are higher than the mobility of c-Si material. However, the mobility values considering the bandgap narrowing are close to the reported mobility values for (n^+) c-Si material (Arora et al, 1982, Caughey et al., 1967). As a result, we believe that the electrical quality of the (n^+) qEpi-Si films falls in the category of c-Si emitters rather than LT Si emitters. This is the major point of this research work.

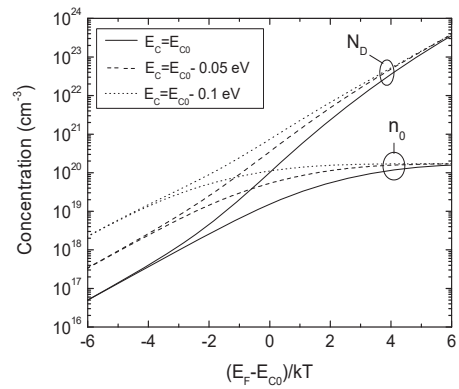

Figure 4. Active doping density (ND) and free electron concentration (n_0) in the c-Si as a function of the Fermi level position calculated for different values for the conduction band edges. The bandgap narrowing at EC of 0, 0.05eV and 0.1eV was assumed in this calculation.

Table II
Electron mobility estimation in the (n^+) qEpi-Si films obtained on mc-Si and CZ-Si wafers

	$N_D=2.5x10^{20}$		$N_D=5x10^{20}$	
BG narrowing	σ =100	σ =450	σ=100	σ=450
0	27.17	122.26	20.16	90.72
50meV	13.52	60.84	10.38	46.71
100meV	7.83	35.24	6.25	28.12

Optical properties of the (n^+) qEpi-Si

Similar to electrical properties, the optical properties of the (n^+) qEpi-Si film deposited on Si substrate are different than the films deposited on glass substrate. We have fabricated some test solar cells with $1cm^2$ area using Al/SiN/(n^+)qEpi-Si/(p)mc-Si/Al structures. The thickness of the SiN layer was 75 nm and the emitter thicknesses was 70 nm. The measured internal quantum efficiencies of the solar cells were employed for the characterization of the films. Figure 5 (a) shows the *IQE* of a sample test solar cell. The drop in the *IQE* in the short wavelength regime, in 375nm – 500 region, is

because of the optical loss in the emitter. If we assume that the emitter contribution in photocurrent is negligible, which is a good approximation for degenerate LT emitters, we can easily extract the effective emitter absorption coefficient (α_e) using α_e=-**ln**(IQE)/t_E, where the t_E is the emitter thickness. Figure 5(b) shows the calculated α_e in short wavelength regime for the solar cell of figure 5(a). It should be noted that the extracted values are not exactly equal to the absorption coefficient of the film because we have not considered the effect of the emitter contribution in *IQE*. Nonetheless, the α_e values of figure 7(b) are in good agreement with the reported values for thick nc-Si films [4]. However, the obtained α_e values in the 375 – 500 nm region are less than the absorption coefficients of (n^+) a-Si films and thin nc-Si films.

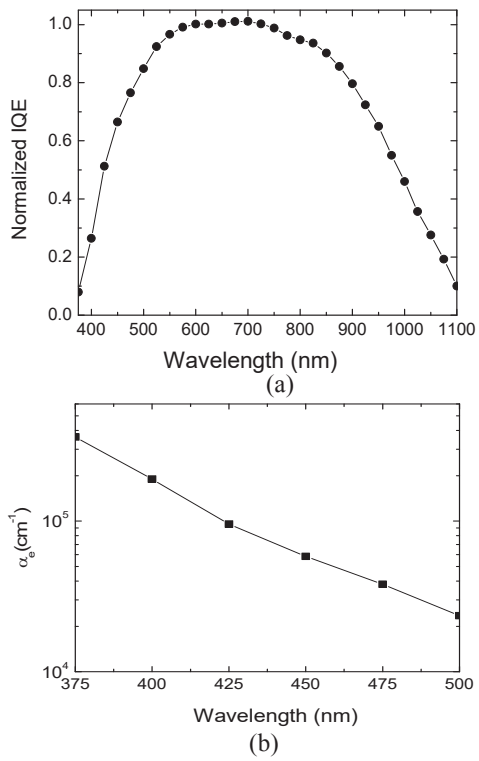

Figure 5. (a) The measured internal quantum efficiency of a fabricated photodiode based on the (n^+)qEpi-Si/(p) mc-Si junction. (b) Extracted effective absorption coefficient of the (n^+) qEpi-Si thin film from the IQE of figure 5(a).

This clearly indicates that the higher crystallinity of the (n^+) qEpi-Si films make then more transparent than the (n^+) a-Si and the thin (n^+) nc-Si film. Considering the fact that the obtained values from IQE measurements are in good agreement with the thick, it can be concluded that the emitter contribution in the photocurrent is negligible.

CONCLUSION

A new kind of (n^+) qEpi-Si emitters with very high conductivities was demonstrated at LTs using PECVD technique. HRTEM pictures from the qEpi-Si films showed that the film benefits from a high degree of crystallinity at the interface region and far from the interface. Using TEM analysis and electrical measurements, it was confirmed that the films have the best structural and electronic quality at the interface and close to the interface region and less quality far from the c-Si substrate. The obtained conductivity values in the range of 100–450 Ω^{-1}cm^{-1} are comparable to the conductivities of the diffused c-Si emitters. Optical absorption of the emitter was characterized at short wavelength region and absorption coefficient of 2x10^5 cm^{-1} was obtained at 400 nm.

ACKNOWLEDGMENT

The authors would like to thank NSERC for funding this project.

REFERENCES

Poissant, Y., Chatterjee, P., and Roca I Cabarrocas, P. 2003, Journal of Applied Physics, **93** 170-174.

Pla, J., Centurioni, E., Summonte, C., Rizzoli, R. 2002, Thin Solid Films **405** 248-255.

Centurioni, E., Iencinella, D., Rizzoli, R., and Zignani, F. 2004, IEEE Transaction on Electron Devices, **51** 1818-1824.

Kerr, M.J., Schmidt, J., and Cuevas, A. 2001, J. Appl. Phys., **89** 3821-3826.

Saha S.C., Rath, J.K., Kshirsagar, S.T., Ray, S. 1997, Journal of Physics D: Applied Physics, **30** 2686–2692

Alpuim, P., Chu, V., Conde, J.P. 2003, J. of Vacuum Science & Technology A **21** 1048-1054.

Farrokh-Baroughi, M., Sivoththaman, S., 2006, Proc. IEEE 4th World Conference on Photovoltaic Energy Conversion, Hawaii, USA

Street, R. A., 1991, Hydrogenated Amorphous Silicon, Cambridge University Press

Luysberg, M., Hapke, P., Carius, R., Finger, F. 1997, Philosophical magazine A **75** 31.

Arora N.D., Hauser, J.R., and Roulston, D.J. 1982, IEEE Transaction on Electron Devices, **29** 292-295

Caughey, D.M., and Thomas, R.E. 1967, Proc. IEEE, **55** 2192-2193.